Group II Intron Protein Localization and Insertion Sites Are Affected by Polyphosphate

Junhua Zhao[1,2,3], Wei Niu[1,2], Jun Yao[1,2,3], Sabine Mohr[1,2,3], Edward M. Marcotte[1,2], Alan M. Lambowitz[1,2,3*]

1 Institute for Cellular and Molecular Biology, University of Texas at Austin, Austin, Texas, United States of America, 2 Department of Chemistry and Biochemistry, University of Texas at Austin, Austin, Texas, United States of America, 3 Section of Molecular Genetics and Microbiology, School of Biological Sciences, University of Texas at Austin, Austin, Texas, United States of America

Mobile group II introns consist of a catalytic intron RNA and an intron-encoded protein with reverse transcriptase activity, which act together in a ribonucleoprotein particle to promote DNA integration during intron mobility. Previously, we found that the *Lactococcus lactis* Ll.LtrB intron-encoded protein (LtrA) expressed alone or with the intron RNA to form ribonucleoprotein particles localizes to bacterial cellular poles, potentially accounting for the intron's preferential insertion in the *oriC* and *ter* regions of the *Escherichia coli* chromosome. Here, by using cell microarrays and automated fluorescence microscopy to screen a transposon-insertion library, we identified five *E. coli* genes (*gppA*, *uhpT*, *wcaK*, *ynbC*, and *zntR*) whose disruption results in both an increased proportion of cells with more diffuse LtrA localization and a more uniform genomic distribution of Ll.LtrB-insertion sites. Surprisingly, we find that a common factor affecting LtrA localization in these and other disruptants is the accumulation of intracellular polyphosphate, which appears to bind LtrA and other basic proteins and delocalize them away from the poles. Our findings show that the intracellular localization of a group II intron-encoded protein is a major determinant of insertion-site preference. More generally, our results suggest that polyphosphate accumulation may provide a means of localizing proteins to different sites of action during cellular stress or entry into stationary phase, with potentially wide physiological consequences.

Introduction

Mobile group II introns, found in bacterial and organelle genomes, consist of a catalytic intron RNA and a multifunctional intron-encoded protein (IEP), which interact to promote RNA splicing and intron mobility [1,2]. The IEP binds to the intron in unspliced precursor RNA, promotes its splicing by stabilizing the catalytically active RNA structure, and remains tightly bound to the excised intron lariat RNA in a ribonucleoprotein particle (RNP) that promotes intron mobility. Mobility occurs by a remarkable mechanism in which the intron RNA inserts (reverse splices) directly into a DNA strand and is reverse-transcribed by the IEP, with the primer being either the opposite DNA strand cleaved by the IEP or a nascent strand at a DNA replication fork (reviewed in [1]). By using this reverse splicing mechanism, mobile group II introns insert at high frequency into specific DNA target sites ("retrohoming") and at low frequency into ectopic sites that resemble the normal homing site ("retrotransposition") [1]. The latter process has led to the wide dispersal of mobile group II introns among bacterial species and also may have been used to invade eukaryotic nuclear genomes, where mobile group II introns are thought to have evolved into spliceosomal introns and non-long-terminal-repeat retrotransposons [2]. Although their DNA integration mechanism has been elucidated, little is known about how mobile group II introns function in a cellular context or about how their mobility is influenced by other cellular processes.

The *Lactococcus lactis* Ll.LtrB intron, which has been used as a model system, is highly mobile not only in *L. lactis* but also in a variety of other bacteria including *Escherichia coli*, where it

has been studied extensively by using the facile genetic and biochemical methods available for that organism [1,3]. The broad host range of the Ll.LtrB intron reflects that RNPs containing only the IEP and intron RNA by themselves carry out the initial reverse splicing and reverse transcription reactions, while the subsequent cDNA integration steps use common host DNA repair functions [4,5].

Ll.LtrB and other mobile group II introns recognize their DNA target sequences by using both the IEP and the base pairing of the intron RNA, with the latter contributing most of the target specificity [6–8]. For Ll.LtrB, these base-pairing interactions involve intron RNA sequences denoted EBS2, EBS1, and δ and complementary DNA target sequences denoted IBS2, IBS1, and δ', extending from position −12 to +2 from the intron-insertion site. (EBS and IBS denote exon- and intron-binding site, respectively.) Because the DNA

Abbreviations: DAPI, 4′,6-diamidino-2-phenylindole; EBS, exon-binding site; GFP, green fluorescent protein; GPPA, guanosine pentaphosphatase A; IBS, intron-binding site; IEP, intron-encoded protein; IPTG, isopropyl β-D-1-thiogalactopyranoside; LB medium, Luria–Bertani medium; LtrA, Ll.LtrB group II intron-encoded protein; *oriC*, chromosomal replication origin; poly(P), polyphosphate; RAM, retrotransposition-activated marker; RNP, ribonucleoprotein particle; RT, reverse transcriptase; TAIL PCR, thermal-asymmetric-interlaced PCR; *ter*, replication terminus; Tp^R, trimethoprim-resistance gene

* To whom correspondence should be addressed. E-mail: lambowitz@mail.utexas.edu

Author Summary

Group II introns are bacterial mobile elements thought to be ancestors of introns—genetic material that is discarded from messenger RNA transcripts—and retroelements—genetic elements and viruses that replicate via reverse transcription—in higher organisms. They propagate by forming a complex consisting of the catalytically active intron RNA and an intron-encoded reverse transcriptase (which converts the RNA to DNA, which can then be reinserted in the host genome). The Ll.LtrB group II intron-encoded protein (LtrA) was found previously to localize to bacterial cellular poles, potentially accounting for the preferential insertion of Ll.LtrB in the replication origin (oriC) and terminus (ter) regions of the Escherichia coli chromosome, which are located near the poles during much of the cell cycle. Here, we identify E. coli genes whose disruption leads both to more diffuse LtrA localization and a more uniform chromosomal distribution of Ll.LtrB-insertion sites, proving that the location of the LtrA protein contributes to insertion-site preference. Surprisingly, we find that LtrA localization in the disruptants is affected by the accumulation of intracellular polyphosphate, which appears to bind basic proteins and delocalize them away from the cellular poles. Thus, polyphosphate, a ubiquitous but enigmatic molecule in prokaryotes and eukaryotes, can localize proteins to different sites of action, with potentially wide physiological consequences.

target site is recognized largely by base pairing of the intron RNA, Ll.LtrB can be retargeted to insert (retrohome) into different chromosomal sites, enabling its development into a gene targeting vector ("targetron") [6,8,9]. Further, an Ll.LtrB intron with randomized EBS2, EBS1, and δ sequences inserts at sites distributed throughout the E. coli genome, analogous to global transposon mutagenesis. Surprisingly, however, we found that although Ll.LtrB could be retargeted to insert efficiently into any region of the E. coli genome, an Ll.LtrB intron with randomized EBS and δ sequences shows a strong proclivity to insert at sites clustered around the bidirectional replication origin (oriC), with 57% of the sites lying within 5% of the chromosome on either side of oriC [10]. Coros et al. [11] studying retrotransposition of the wild-type Ll.LtrB intron into ectopic sites in E. coli observed a similar clustering of insertion sites in both the oriC and the ter regions.

Previously, we hypothesized that the preferential insertion of the Ll.LtrB intron into the oriC and ter regions of the E. coli chromosome might reflect the intracellular localization of Ll.LtrB RNPs [12]. In E. coli, the oriC and ter regions are localized near the cellular poles during much of the cell cycle [13,14], and we found by using both LtrA fusions with green fluorescent protein (GFP) and immunofluorescence microscopy that LtrA expressed alone or with Ll.LtrB RNA to form RNPs localizes to the cellular poles in both E. coli and L. lactis [12]. Further analysis in E. coli showed that the bipolar localization of LtrA occurs over a wide range of cellular growth rates and LtrA expression levels, is independent of oriC function, and occurs in anucleate cells, suggesting that LtrA simply is not forced to the poles by nucleoid occlusion [12]. We also found that LtrA expression in E. coli interferes with the polar localization of coexpressed Shigella flexneri IcsA protein, suggesting competition for a common localization determinant [12]. Beauregard et al. [15] found that the polar localization of LtrA is maintained in E. coli mutants with defects in nucleoid condensation, chromosome partitioning,

and DNA replication, and as expected from its continued pole localization, Ll.LtrB retrotransposition sites remained clustered in the oriC and ter regions in such mutants.

While the above findings are consistent with the possibility that the bipolar localization of LtrA is responsible for the clustering of Ll.LtrB-insertion sites in the oriC and ter regions of the E. coli chromosome, to prove this connection, it is necessary to obtain mutations that change LtrA's intracellular localization and show that they correspondingly change the chromosomal distribution of Ll.LtrB-insertion sites. However, mutations that affect the polar localization of proteins in E. coli have been difficult to find. Nilsen et al. [16] manually screened ~7,000 E. coli mutants for altered localization of the S. flexneri IcsA protein. The only mutant identified was in the mreB gene, which encodes a bacterial actin homologue required for maintenance of the cell's rod shape, and in this case, an IcsA/GFP fusion protein simply showed multiple foci in a portion of the spherical mutant cells instead of two foci at poles.

Here, we used automated fluorescence microscopy of cell microarrays [17] to screen a transposon-insertion library for mutants with altered LtrA localization. We identified five E. coli genes (gppA, uhpT, wcaK, ynbC, and zntR) whose disruption leads to both a more diffuse intracellular distribution of LtrA and a more uniform genomic distribution of Ll.LtrB-insertion sites, indicating that group II intron protein localization is a major determinant of insertion-site preference. Surprisingly, we find that the common factor affecting LtrA localization in these disruptants is the accumulation of intracellular polyphosphate poly(P). We confirmed this connection by analyzing ppx disruptants, which lack the exopolyphosphatase that degrades poly(P), and found that disruptants that accumulate poly(P) also show delocalization of other pole-localized basic proteins (Neurospora crassa CYT-18 and E. coli XapR). Our findings show that poly(P), which accumulates in response to cell stress or entry into stationary phase, can localize proteins to different sites of action, with potentially wide physiological consequences.

Results

Cell Microarray Screen for E. coli Mutants with Altered LtrA Localization

To screen for E. coli mutants with altered LtrA localization, we constructed a library of mariner transposon insertions in E. coli HMS174(DE3), a standard host strain that contains an integrated λDE3 prophage with an isopropyl β-D-1-thiogalactopyranoside (IPTG)-inducible T7 RNA polymerase for Ll.LtrB intron expression (see Materials and Methods section). For screening, the library was transformed with intron-donor plasmid pACD2X-GFP/LtrA, which uses a T7lac promoter to express an Ll.LtrB-ΔORF intron with short flanking exons, plus a GFP/LtrA fusion protein downstream of the 3′ exon (E2; Figure 1A). This configuration gives high intron mobility frequencies and permits independent manipulation of the intron RNA and IEP. We showed previously that GFP/LtrA expressed from this plasmid is active in promoting both RNA splicing and intron mobility [12].

The library in 96-well plate format was arrayed onto microscope slides and screened for mutants with altered GFP/LtrA localization by automated fluorescence microscopy (Figure 1B; see Materials and Methods section). The images
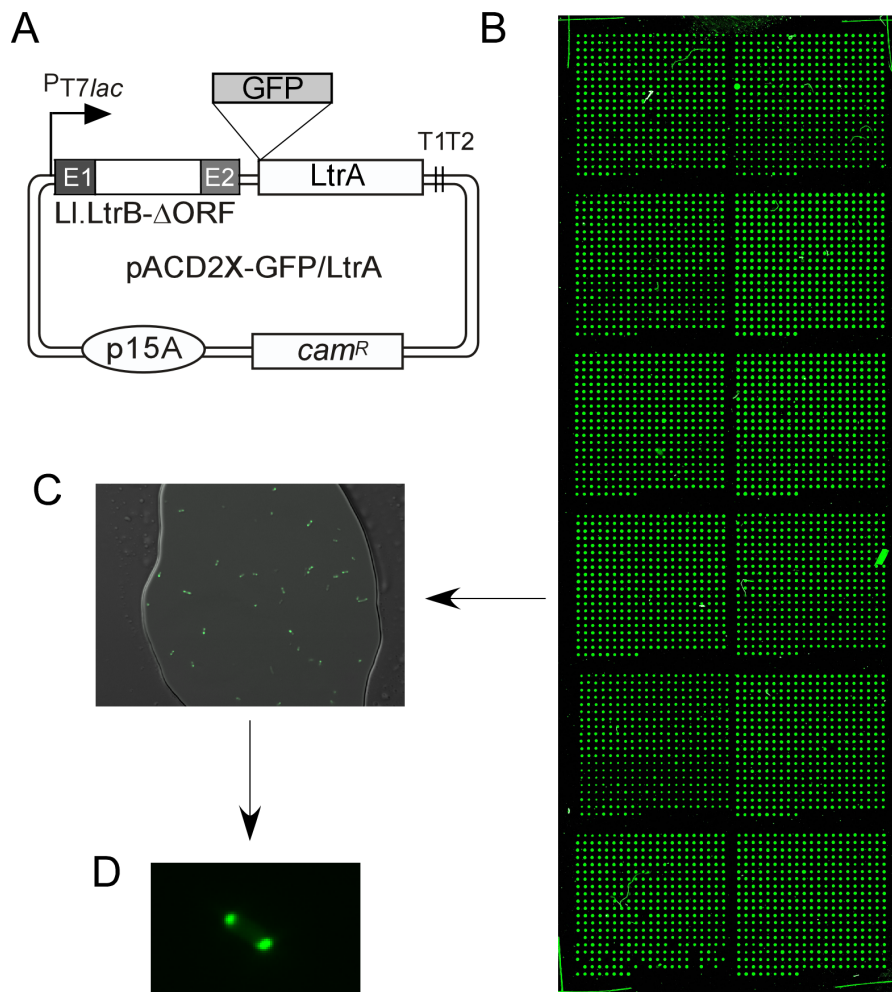
Figure 1. Intron-Expression Plasmid and Cell Microarrays Used to Identify *E. coli* Disruptants with Altered GFP/LtrA Localization

(A) pACD2X-GFP/LtrA uses a T7 *lac* promoter to express the Ll.LtrB-ΔORF intron with short flanking exons, followed by a GFP/LtrA fusion protein [12]. E1 and E2 are 5′ and 3′ exons, respectively, and T1 and T2 are *rrnB* transcription terminators.

(B) Wide-field light scattering image of a cell microarray. A *mariner* transposon-insertion library of *E. coli* HMS174(DE3) cells carrying pACD2X-GFP/LtrA was arrayed onto microscope slides like that shown and screened by automated fluorescence microscopy to identify mutants with altered GFP/LtrA localization patterns (see Materials and Methods section).

(C) Close-up of a spot from the cell microarray.

(D) Higher magnification view of the same spot focusing on an *E. coli* cell with the wild-type bipolar GFP/LtrA localization pattern.

doi:10.1371/journal.pbio.0060150.g001

were stored and then examined individually to characterize GFP/LtrA localization patterns (Figure 1C and 1D). A total of 9,600 disruptants were screened under two different Ll.LtrB induction conditions (overnight with 500 μM IPTG at 30 °C or 100 μM IPTG at 37 °C). Of 277 initial candidates, 36 showed similarly altered GFP/LtrA localization patterns in duplicate arrays, and five that showed the most strongly altered GFP/LtrA localization patterns in liquid culture were studied further.

Identification of *E. coli* Genes Affecting LtrA Localization

The *mariner* transposon-insertion sites in the five disruptants were amplified and sequenced via thermal-asymmetric-interlaced (TAIL) PCR and found to be in the *gppA*, *uhpT*, *wcaK*, *ynbC*, and *zntR* genes. *gppA* encodes guanosine pentaphosphatase A, which removes the 5′ phosphate from pppGpp to produce the stringent response regulator, ppGpp ("magic spot") [18]; *uhpT* encodes a hexose phosphate transport component [19]; *wcaK* is a predicted colanic acid

biosynthesis pyruvyl transferase [20]; *ynbC* encodes a 585-amino-acid ORF of unknown function [21]; and *zntR* encodes a zinc-responsive transcriptional regulator [22]. In each disruptant, the transposon-insertion site was confirmed by additional PCRs to amplify and sequence both the 5′- and the 3′-transposon-integration junctions (Figure S1) and by Southern hybridization, which also showed that each strain contains a single transposon insertion (Figure S2). Immunoblots showed that the GFP/LtrA expression levels in the disruptants are similar to or lower than those in the wild-type strain, with the expression level particularly low in the *ynbC* disruptant (Figure S3). These findings indicate that the disruptions affect GFP/LtrA localization over a wide range of protein expression levels. *gppA* and *uhpT* are in single gene transcription units, and *zntR* is the last gene of a two-gene operon, while *ynbC* and *wcaK* are upstream genes in operons whose disruption could exert polar effects on downstream genes [23].
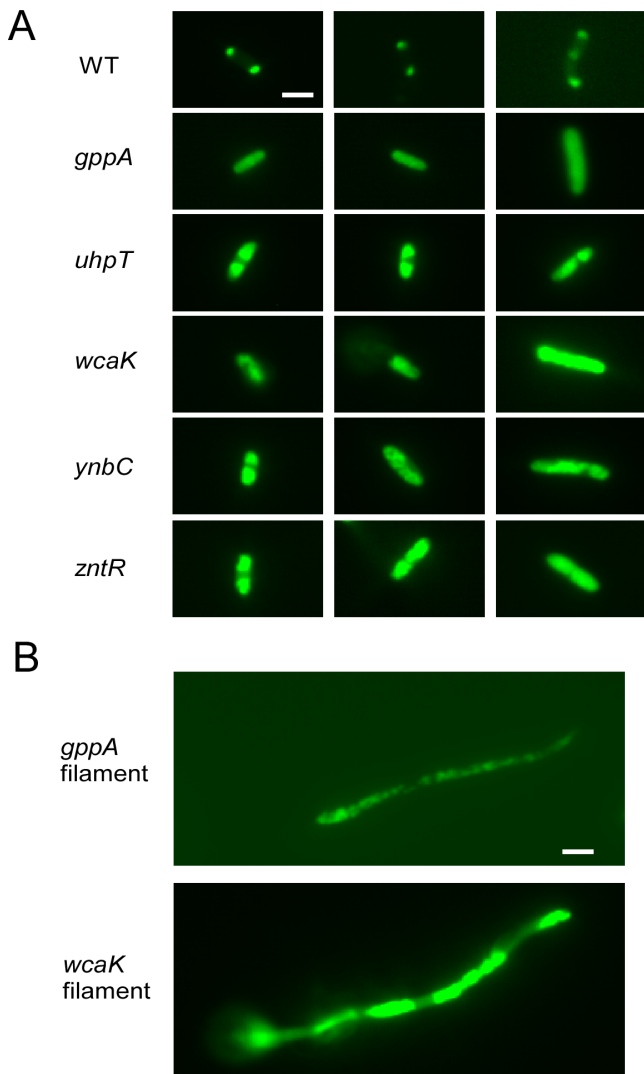
Figure 2. Fluorescence Microscopy of GFP/LtrA in Wild-Type *E. coli* and Disruptants with Altered GFP/LtrA Localization Patterns

Wild-type HMS174(DE3) (WT) and disruptants containing pACD2X-GFP/LtrA were induced with 500 μM IPTG overnight at 30 °C. For each strain, ≥200 cells were examined by fluorescence microscopy, as described in the Materials and Methods section, and the proportions of cells with different LtrA localization patterns are summarized in Table 1, top. The localization patterns shown in the figure represent the most common pattern for each strain. Bar = 2 μm.
(A) Wild-type cells showing bipolar GFP/LtrA localization and disruptants showing diffuse GFP/LtrA localization patterns.
(B) Filamentous *gppA* and *wcaK* cells showing multiple GFP/LtrA foci, diffuse patches, or a combination of the two.
doi:10.1371/journal.pbio.0060150.g002

Intracellular Localization of LtrA in the Disruptants

To characterize their GFP/LtrA localization patterns, the wild-type and disruptant strains were grown in liquid culture, and GFP/LtrA expression was induced overnight with 500 μM IPTG at 30 °C, one of the induction conditions used for screening the transposon-insertion library. GFP/LtrA localization patterns in ≥200 randomly selected cells of each strain were then analyzed by fluorescence microscopy (Figure 2 and Table 1, top). As found previously, in the wild-type strain, a high proportion of the cells (81.2%) showed polar localization of LtrA. Such cells contain one or two small, discrete GFP/LtrA foci at their poles, with elongated cells,

presumably those ready for division, typically showing a third focus in the middle. Only 2.8% of the wild-type cells showed diffuse GFP/LtrA localization patterns. In wild type as well as the disruptants, ~20% of cells did not show GFP/LtrA fluorescence detectable above background.

In comparison to the wild-type strain, each of the disruptants showed a substantially increased proportion of cells with more diffuse GFP/LtrA localization patterns (26.4–46.1%), which were classified into two types: completely diffuse (C), with GFP/LtrA uniformly distributed throughout the cell, or partially diffuse (P), with GFP/LtrA spread out from the poles but leaving a clear area in the middle of the cell (percentages of C and P are indicated in parentheses in Table 1). The *gppA* disruptant was the most strongly affected, with only 20.5% of the cells still showing polar GFP/LtrA localization, 39.5% showing partially or completely diffuse fluorescence, and 16.9% filamentous cells with multiple foci and/or irregular diffuse patches of GFP/LtrA fluorescence (Figure 2 and Table 1, top). The *wcaK* disruptant also showed an increased proportion of filamentous cells (18.6%), while the remaining three disruptants showed few or no filamentous cells. The ratio of cells with completely or partially diffuse LtrA localization differed for each of the disruptants, being highest for the *zntR* disruptant and lowest for the *uhpT* disruptant. When Ll.LtrB intron expression was induced under the higher temperature conditions (overnight, 100 μM IPTG, 37 °C), we observed similar GFP/LtrA localization patterns, but the proportions of cells showing completely or partially diffuse fluorescence shifted in some cases (Table S1).

Although their cellular phenotypes are heterogeneous, PCR using primers flanking the target gene showed that cultures of four of the disruptants (*gppA*, *uhpT*, *wcaK*, and *ynbC*) were homogenous for the disrupted allele, while the fifth (*zntR*) contained predominantly the disrupted allele but also showed a light band (star) comigrating with that for the wild-type allele (Figure S4). This light band was found by sequencing to contain a 4-bp insertion at the transposon-insertion site in the middle of the ORF and is presumably a null allele resulting from transposon excision. Thus, in all cases, the heterogeneous cellular phenotype is not due to persistence of the wild-type allele.

Intron Mobility Frequencies in the Disruptants

Next, we tested whether the disruptions affect intron mobility frequencies. For these experiments, we used an Ll.LtrB-ΔORF intron that had been retargeted by modification of its EBS and δ sequences to insert at a site within the *E. coli lacZ* gene (LacZ-1063a) so that the intron integration frequency could be scored simply by blue–white screening (see Materials and Methods section and Figure S5). Intron-donor plasmid pACD2X expressing the retargeted intron was transformed into the wild-type and disruptant strains and induced with IPTG at 30 or 37 °C prior to plating the cells on Luria–Bertani (LB) medium containing X-Gal. As summarized in Figure 3, at both temperatures, Ll.LtrB-ΔORF intron mobility frequencies in the disruptants were somewhat higher than those in the wild-type strain (68–96% compared to 47–51%). Immunoblots of proteins isolated from the induced cells showed slightly reduced levels of LtrA protein in all cases (69–78% wild type; Figure 3B), indicating that the increased mobility frequencies simply are not due to higher protein expression levels. Possible reasons for the increased chromo-

Table 1. GFP/LtrA Localization in Wild-Type and Mutant Strains

Strain	GFP/LtrA Localization Pattern (%)			
	Polar	Diffuse (C/P)	Filaments	No Fluorescence
WT	81.2	2.8 (0.3/2.5)	0	16.0
gppA	20.5	39.5 (24.1/15.4)	16.9	23.1
uhpT	32.5	42.9 (13.2/29.7)	1.1	23.5
wcaK	36.7	26.4 (13.2/13.2)	18.6	18.3
ynbC	27.5	46.1 (17.9/28.2)	0	26.4
zntR	35.7	46.0 (36.3/9.7)	0.7	17.6
relA	72.2	4.2 (1.4/2.8)	11.1	12.5
relA/spoT*	69.2	6.3 (4.3/2.0)	0	24.5
ppk	64.8	6.2 (2.6/3.6)	0.6	28.4
ppx	45.6	27.4 (10.2/17.2)	4.7	22.3
ppk*	73.8	3.8 (2.2/1.6)	0.4	22.0
ppx*	60.6	18.7 (10.6/8.1)	0.7	20.0

Cells containing pACD2X-GFP/LtrA were induced with 500 μM IPTG at 30 °C overnight, and ≥200 cells of each strain were examined by fluorescence microscopy to characterize GFP/LtrA localization patterns. Patterns are characterized as polar, diffuse, filamentous, or no detectable fluorescence above background. For cells with diffuse GFP/LtrA localization, the percentages showing completely (C) or partially (P) diffuse fluorescence patterns are indicated in parentheses. Filamentous cells showed either multiple foci, diffuse GFP/LtrA fluorescence, or a combination of the two. Asterisks indicate strains obtained from GenoBase, with genetic background different from *E. coli* HMS174(DE3).
doi:10.1371/journal.pbio.0060150.t001

somal insertion frequencies in the disruptants are discussed below (see Discussion section).

Chromosomal Distribution of Ll.LtrB Intron-Insertion Sites in Wild-Type and Disruptant Strains

Having demonstrated that the Ll.LtrB-ΔORF intron remains mobile in the disruptants, we next examined whether the changes in LtrA localization patterns are correlated with changes in the genomic distribution of Ll.LtrB-insertion sites. As done previously to analyze insertion-site preference [10], we used a donor plasmid library that expresses Ll.LtrB-ΔORF introns with randomized target site recognition (EBS2, EBS1, and δ) sequences plus a Tp^R retrotransposition-activated marker (RAM) to detect chromosome integrations. This marker consists of a small trimethoprim-resistance (Tp^R) gene inserted within the intron in the orientation opposite to intron transcription but interrupted by a small, self-splicing group I intron (the phage T4 *td* intron) in the forward orientation. During retrohoming via an RNA intermediate, the group I intron is spliced, reconstituting the marker and enabling the selection of cells containing integrated introns by trimethoprim resistance. The Tp^R colonies were isolated and analyzed by TAIL PCR and sequencing to identify the intron-insertion sites.

The chromosomal distributions of Ll.LtrB-ΔORF intron-insertion sites in wild-type HMS174(DE3) and the disruptants are shown in Figure 4, with the previous distribution for wild-type HMS174(DE3) from Zhong et al. [10] shown for comparison. The two sets of data for the wild-type strain are in close agreement, showing Ll.LtrB intron-insertion sites strongly clustered around *oriC* (blue bars; Figure 4A and 4B). By combining the two data sets for the wild-type strain, we defined the region around *oriC* containing clustered Ll.LtrB-insertion sites as encompassing minutes 69–90 of the *E. coli* chromosome (21% of the genome).

In the wild-type strain, the proportion of Ll.LtrB-insertion sites in the *oriC* region defined as above was 75% in the previous work (Figure 4A) and 78% in the present work (Figure 4B), strikingly higher than 21% expected for random

integration. By contrast, in the disruptants only 35–53% of the Ll.LtrB-insertions sites were located in the *oriC* region, with the lowest proportions being found in the *zntR* and *ynbC* disruptants (35% and 38%, respectively; Figure 4C–G). The differences in distribution patterns were statistically significant at $p < 0.001$, calculated by χ-square test. These findings show that the more diffuse intracellular localization of GFP/LtrA in the disruptants is in fact correlated with a more uniform distribution of Ll.LtrB-insertion sites.

Clues from the gppA Disruptant: GFP/LtrA Localization Is Not Affected by Decreased Synthesis of Magic Spot, but Is Affected by Polyphosphate Accumulation

Among the genes whose disruption results in altered GFP/LtrA localization, the best characterized is *gppA*, which encodes guanosine pentaphosphatase A (GPPA). This enzyme has two functions: it dephosphorylates pppGpp to produce ppGpp ("magic spot"), and it processively hydrolyzes intracellular poly(P), liberating orthophosphate [18].

To test whether the altered LtrA localization pattern in the *gppA* disruptant is due to impaired synthesis of magic spot, we examined LtrA localization in two other mutants that affect the synthesis of magic spot in different ways: a *relA* disruptant derived from wild-type HMS174(DE3) by targetron mutagenesis (Figure S5) and a previously isolated *relA/spoT** double mutant obtained from GenoBase [24]. (Note that strains obtained from GenoBase were derivatized with λDE3 for intron expression and are denoted with an asterisk to indicate different genetic background.) Both the *relA* and the *relA/spoT** mutants still showed predominantly polar localization of GFP/LtrA (72.2% and 69.2% of cells, respectively), with only small proportions of cells (4.2% and 6.3%, respectively) showing diffuse GFP/LtrA localization (Figure 5A and Table 1, bottom). Thus, impaired ability to produce ppGpp does not strongly affect LtrA localization. The mobility frequency of the Ll.LtrB-ΔORF intron assayed by targeted integration into the *lacZ* gene as above was increased in the *relA* disruptant and decreased in the *relA/spoT** mutant compared to the wild-type strain (Figure 5B). The lower
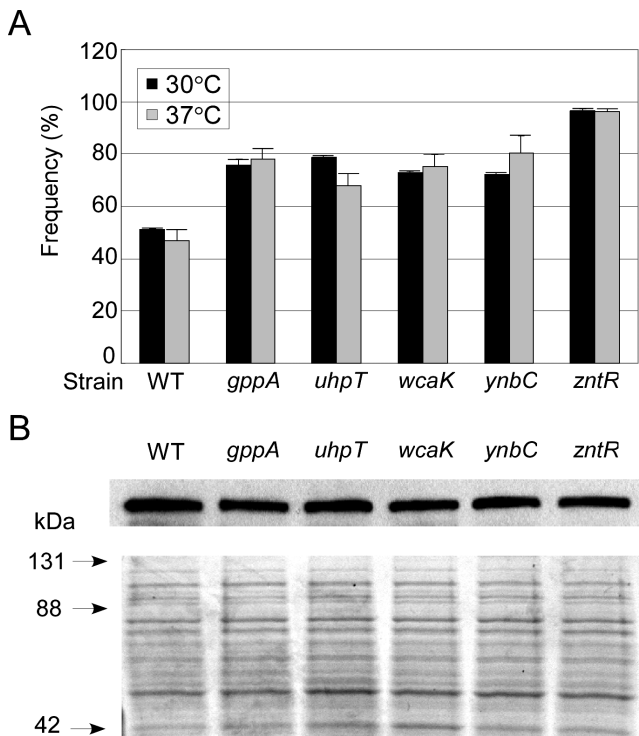
A

B

Figure 3. Ll.LtrB-ΔORF Intron Mobility Frequencies in Wild Type and Disruptants with Altered GFP/LtrA Localization Patterns

(A) Mobility frequencies. Donor plasmid pACD2X containing an Ll.LtrB-ΔORF intron retargeted to insert at a site in the *E. coli lacZ* gene (between nucleotide residues 1062 and 1063, antisense strand; Figure S5) was transformed into the indicated strains and induced with 500 μM IPTG for 0.5 h at 30 °C (black bars) or 100 μM IPTG for 1 h at 37 °C (gray bars). The cells were then plated on LB medium containing X-Gal, and the *lacZ* integration frequency was calculated as the percentage of white colonies. The bar graphs show the mean for three independent assays, with the error bars indicating the standard deviation.

(B) LtrA expression levels in the cultures used for mobility assays after induction with IPTG at 30 °C. Top, immunoblot probed with an anti-LtrA antibody preparation. Bottom, a parallel gel stained with Coomassie blue. Arrows to the left of the gel indicate positions of size markers (Kaleidoscope Prestained Standard; Bio-Rad).

doi:10.1371/journal.pbio.0060150.g003

intron mobility frequency in the *relA/spoT** mutant could be due to the *relA/spoT* mutations, the different genetic background, or a combination of the two.

The alternate possibility was that GFP/LtrA localization in the *gppA* disruptant might be due to the accumulation of intracellular poly(P). To test this possibility, we used targetron mutagenesis to disrupt the *E. coli* HMS174(DE3) *ppk* and *ppx* genes, which encode polyphosphate kinase and exopolyphosphatase, respectively [25,26] (Figure S5). The *ppk* and *ppx* genes are expressed from the same operon, with *ppk* upstream of *ppx*. Thus, the disruption of *ppk* is expected to affect the expression of both genes and lead to decreased levels of intracellular poly(P), while the disruption of *ppx* should affect only the expression of that gene and lead to accumulation of poly(P) [26,27].

The *ppx* disruptant, which we confirmed below accumulates poly(P), did in fact show a substantially increased proportion of cells with more diffuse GFP/LtrA localization (27.4%), while the *ppk* disruptant, expected to have decreased levels of poly(P), showed predominantly the normal bipolar GFP/LtrA localization pattern (Figure 5A and Table 1, bottom). Similar

results were obtained with independently constructed *ppx* and *ppk* deletions from the Keio collection obtained from GenoBase (i.e., more diffuse GFP/LtrA localization in the *ppx** deletion (18.7%) and predominantly bipolar GFP/LtrA localization in the *ppk** deletion (Table 1, bottom)). In both the *ppk* and the *ppx* disruptants, the mobility frequency of the Ll.LtrB-ΔORF intron assayed by targeted integration into the *lacZ* gene was increased relative to the wild-type strain, with the increases more pronounced if normalized to the LtrA expression level (Figure 5B and 5C). We conclude from these findings that the common feature correlated with the more diffuse LtrA localization in the *gppA* and *ppx* disruptants is the accumulation of intracellular poly(P).

Intracellular Distribution of Poly(P) in Wild-Type and Disruptant Strains

To investigate further the relationship between poly(P) accumulation and GFP/LtrA localization, we used fluorescence microcopy to examine the intracellular localization of poly(P) detected by 4′,6-diamidino-2-phenylindole (DAPI) staining in the wild-type strain and the *gppA* and *ppx* disruptants expressing GFP/LtrA. Under fluorescence microscopy with excitation at 360 nm, DAPI bound to poly(P) emits at 550 nm and appears yellow or orange, while DAPI bound to DNA emits at 490 nm and appears blue [28].

In wild-type HMS174(DE3) under standard GFP/LtrA induction conditions at 30 °C, 16.5% of the cells showed detectable poly(P) fluorescence localized in discrete foci, mainly at the cell poles (P), another 8.9% showed more diffuse poly(P) fluorescence (D), and the remainder (74.6%) showed no detectable poly(P) fluorescence (N), likely reflecting at least in part the sensitivity of the detection method (Figure 6A). The localization of poly(P) in discrete foci ("volutin granules") at the cellular poles has been found previously in other bacteria [29–31].

By contrast, under the same conditions, both the *gppA* and the *ppx* disruptions, which lack enzymes involved in poly(P) degradation, showed substantially increased proportions of cells with detectable poly(P) fluorescence (55.9% and 61.1%, respectively; Figure 6A). Further, in a high proportion of *gppA* and *ppx* disruptant cells, poly(P) was no longer present in discrete foci but was instead dispersed throughout the cell (44.4% and 25.4%, respectively, excluding filamentous *gppA* cells). Conversely, the *ppk* disruptant, which lacks the major poly(P) biosynthetic enzyme, shows a reduced proportion of cells with detectable poly(P) fluorescence, which was localized again mainly at or near the cell poles (6.6%; Figure 6A). The residual poly(P) in the *ppk* disruptant may be synthesized by an alternate pathway [32]. Similar differences in poly(P) localization between the wild-type and the disruptant strains were observed after IPTG induction in strains carrying the empty vector, indicating that poly(P) accumulation in the disruptants is not due to expression of GFP/LtrA (unpublished data).

Importantly, although the *gppA* and *ppx* disruptants have heterogeneous cellular phenotypes, poly(P) accumulation and dispersed GFP/LtrA localization were correlated strongly in individual cells. Thus, for the *gppA* disruptant, 90% of the doubly fluorescent cells with diffuse poly(P) localization showed diffuse GFP/LtrA localization, and 96% with diffuse GFP/LtrA localization showed diffuse poly(P) fluorescence. Similarly, in the *ppx* disruptant, 89% of the doubly
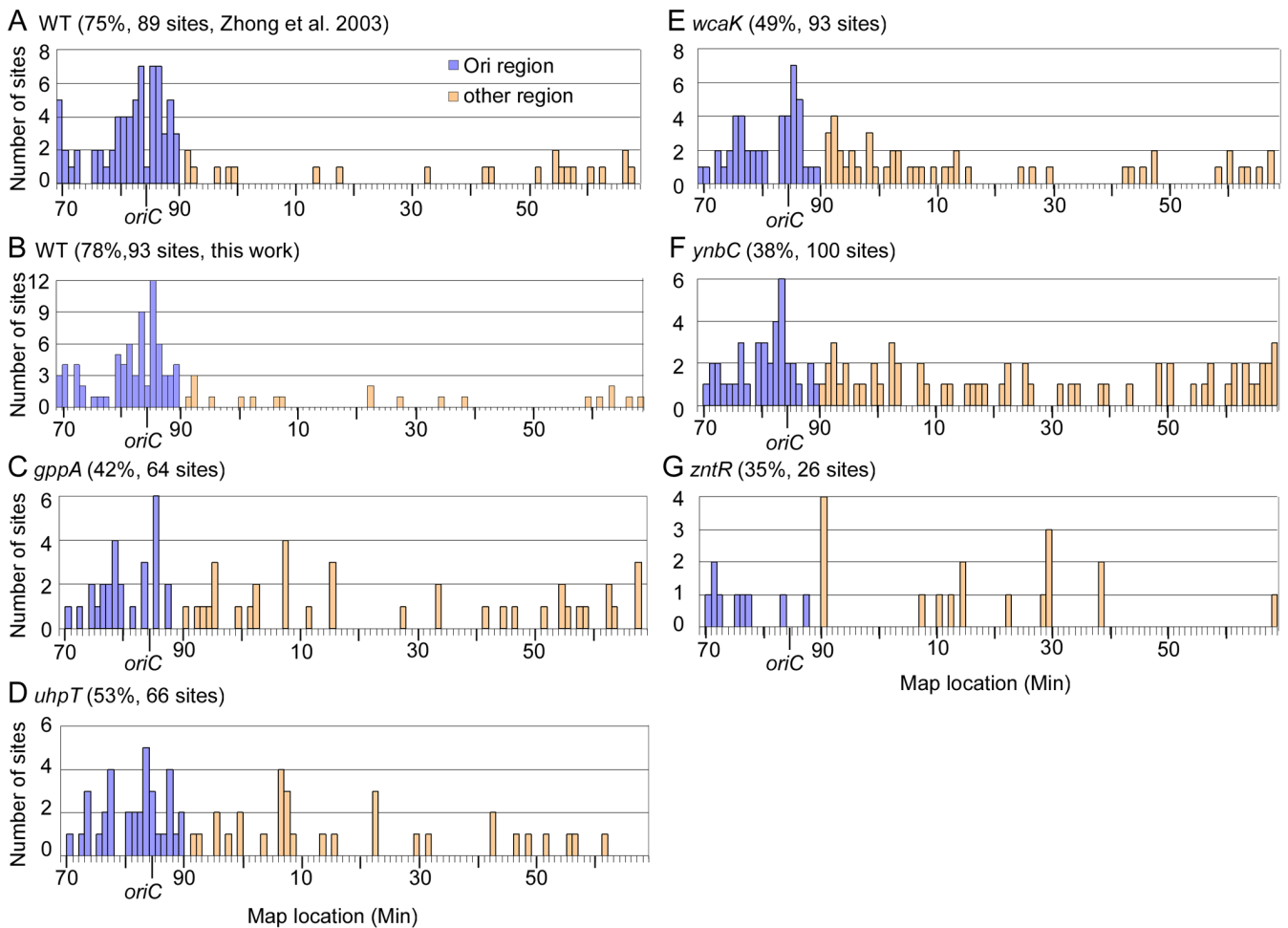
Figure 4. Ll.LtrB-ΔORF Intron Insertion Site Distribution in Wild Type and Disruptants with Altered GFP/LtrA Localization Patterns

Wild-type HMS174(DE3) and disruptants showing altered GFP/LtrA localization patterns were transformed with pACD3-Tp^R-RAM containing a library of Ll.LtrB-ΔORF introns with randomized EBS1, EBS2, and δ sequences plus a Tp^R-RAM in intron domain IV. After induction, cells were plated on medium containing trimethoprim to select cells containing integrated Ll.LtrB introns carrying the activated Tp^R-RAM, and insertion sites in randomly selected colonies were identified by TAIL PCR and sequencing.

(A and B) Chromosomal distribution of Ll.LtrB-ΔORF intron-insertion sites in wild-type *E. coli* HMS174(DE3) (WT) from Zhong et al. [10] and this work, respectively.

(C–G) Chromosomal distribution of Ll.LtrB-ΔORF intron-insertion sites in the indicated disruptants with more diffuse GFP/LtrA localization patterns. Blue bars represent insertion sites within the 69–90 minute region encompassing *oriC* (21% of the genome), and peach bars represent insertion sites outside this region. The numbers above the graphs show the percentage of sites in the *oriC* region and the total number of independent sites sequenced for each strain. In two separate inductions with the *zntR* disruptant, a single but different insertion site outside the *oriC* region was found repeatedly among sequenced colonies (21/26 at 1325864 in *btuR* and 21/50 at 4199340 in *zraP*), resulting in a smaller number of independent sites sequenced for that strain. Such a repeated occurrence could reflect either that hot spots exist for intron integration or that the integration occurred prior to or early in induction and was amplified in the culture by cell division. In the other strains, two to three insertion sites, which differed in each strain, were repeated two to four times among sequenced colonies. In all cases, such repeated sites were counted as a single site in the analysis shown. If the repeated sites were counted as independent events, then the proportions in the *oriC* region would be WT, 79%; *gppA*, 45%; *uhpT*, 47%; *wcaK*, 51%; *ynbC*, 31%; and *zntR*; 14%.

doi:10.1371/journal.pbio.0060150.g004

fluorescent cells with diffuse poly(P) localization showed diffuse GFP/LtrA localization, and 88% with diffuse GFP/LtrA localization showed diffuse poly(P) localization. Further, in a high proportion of the doubly fluorescent cells, the poly(P) and GFP/LtrA fluorescence were either overlapping (94.7% and 87.9% in the *gppA* and *ppx* disruptants, respectively) or completely colocalized (78.4% and 45.5% in the *gppA* and *ppx* disruptants, respectively; Figure 6C). This degree of colocalization supports the hypothesis that the altered GFP/LtrA localization is due to the binding of the basic LtrA protein to the negatively charged poly(P). Those cells in which both poly(P) and GFP/LtrA are dispersed but not completely

colocalized could reflect that poly(P) associated with LtrA dissociates or is degraded after the protein is dispersed, that some poly(P) bound to LtrA is less than the concentration limit required for fluorescence detection with DAPI, or that the GFP tag is clipped, rendering some proportion of LtrA nonfluorescent.

After the above findings, we also re-examined the wild-type strain, where 2.8% of the cells showed diffuse GFP/LtrA localization (Table 1, top). Strikingly, even in wild type, where only a small proportion of cells is affected, diffuse GFP/LtrA localization was correlated again with the accumulation and dispersal of poly(P) (88% of wild-type cells with diffuse GFP/
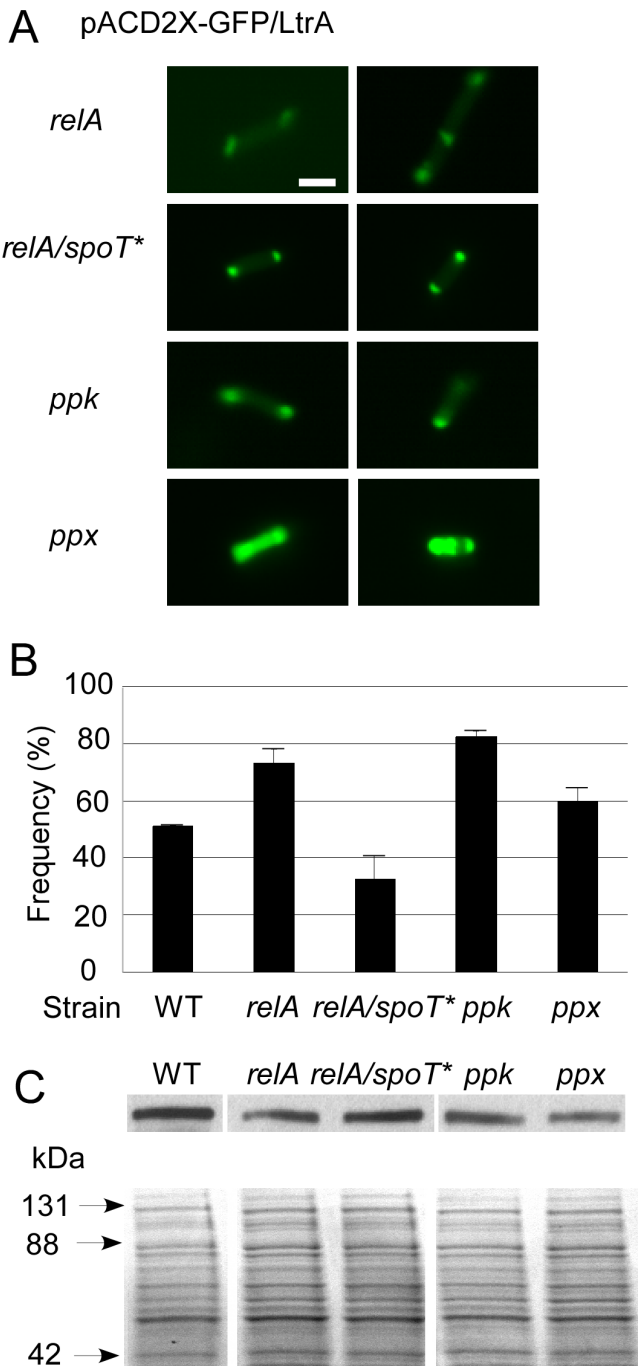
A   pACD2X-GFP/LtrA

relA

relA/spoT*

ppk

ppx

B

C

Figure 5. GFP/LtrA Localization Patterns and Intron Mobility Frequencies in Mutants Affecting Magic Spot and Poly(P) Accumulation

(A) Fluorescence microscopy of GFP/LtrA localization in a *relA* disruptant and a *relA/spoT** mutant defective in synthesis of magic spot and in *ppk* and *ppx* disruptants, which inhibit the synthesis and degradation of poly(P), respectively. Cells containing pACD2X-GFP/LtrA were induced with 500 μM IPTG overnight at 30 °C. For each strain, ≥200 cells were examined by fluorescence microscopy, and the proportions of cells with different LtrA localization patterns are summarized in Table 1, bottom. The localization patterns shown in the figure represent the most common pattern for each strain. Bar = 2 μm.

(B) Mobility frequencies of the LI.LtrB-ΔORF intron in different strains determined by using a chromosomal *lacZ* gene disruption assay (see Figure 3 and Materials and Methods section). The bar graphs show the mean for three independent assays, with the error bars indicating the standard deviation.

(C) LtrA expression levels from cultures used in the mobility assay. Top, an immunoblot probed with an anti-LtrA antibody preparation. Bottom,

a parallel gel stained with Coomassie blue (all lanes from the same gel). Arrows to the left of the gel indicate positions of size markers (Kaleidoscope Prestained Standard; Bio-Rad).

Asterisks indicate that the strain was obtained from GenoBase.

doi:10.1371/journal.pbio.0060150.g005

LtrA showed dispersed poly(P), and 83% with dispersed poly(P) showed diffuse GFP/LtrA. The accumulation of poly(P) in a small proportion of wild-type cells is likely due to cell stress, which triggers poly(P) synthesis [33]. Collectively, these findings suggest that the more diffuse intracellular localization of GFP/LtrA results from the accumulation of poly(P), which binds to LtrA and delocalizes it away from the cell poles.

All the Other Disruptants with Diffuse GFP/LtrA Localization Also Accumulate Poly(P)

The remaining four disruptants (*uhpT*, *wcaK*, *ynbC*, and *zntR*) with more diffuse GFP/LtrA localization do not involve genes that are known to function in poly(P) metabolism. However, the above findings raised the possibility that they might also accumulate poly(P) as a result of cell stress caused by the disruptions. Fluorescence microscopy of DAPI-stained cells revealed that this is in fact the case, with all four of the above disruptants in the HMS174(DE3) genetic background showing an increased proportion of cells with higher and more dispersed poly(P) fluorescence (Figure 6B). By contrast, strains having deletions of the same four genes (*uhpT**, *wcaK**, *ynbC**, and *zntR**) in the Keio genetic background did not accumulate poly(P) and correspondingly did not exhibit altered GFP/LtrA localization patterns (unpublished data). The likely explanation is that their different genetic background makes the Keio strains less prone to cell stress caused by these mutations and/or less prone to accumulate poly(P) in response to cell stress than in the HMS174(DE3) background. In comparison to the *ppx* disruption in the HMS174(DE3) background (Figure 6), the *ppx** deletion in the Keio genetic background also showed less detectable poly(P) accumulation (1.0% P, 6.0% D, 93.0% N) and correspondingly had a more muted effect on GFP/LtrA localization (Table 1, bottom). We conclude that poly(P) accumulation is the common factor correlated with altered GFP/LtrA localization in all of the strains analyzed here.

Poly(P) Binds to LtrA and Inhibits Its Reverse Transcriptase Activity

To test directly whether poly(P) binds to LtrA, we examined its effect on the electrophoretic mobility of the LtrA protein in a nondenaturing polyacrylamide gel (Figure 7A). In the absence of poly(P), the LtrA protein, which is highly positively charged (calculated pI = 9.6), could not migrate toward the positive pole and failed to enter the gel. By contrast, with increasing concentrations of poly(P), an increasing proportion of LtrA entered the gel and migrated toward the positive pole, indicating complex formation. Control lanes (right) show that the highest concentration of poly(P) tested had no effect on the electrophoretic mobility of an acidic protein, bovine serum albumin (pI = 4.6), run in the same gel. Figure 7B extends these findings by showing that equimolar poly(P) completely inhibited the reverse transcriptase (RT) activity of LtrA. Poly(P) also inhibited the RT activity of Moloney murine leukemia virus and Superscript
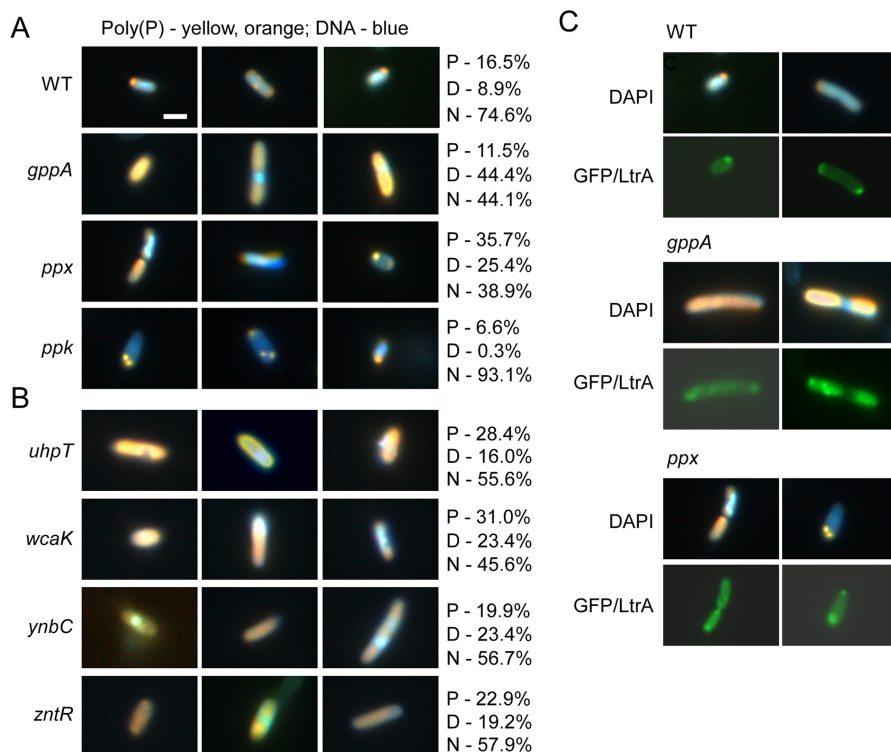
Figure 6. Fluorescence Microscopy of Poly(P) and GFP/LtrA Localization in Wild Type and Disruptants

Wild-type HMS174(DE3) (WT) and disruptants containing pACD2X-GFP/LtrA were induced with 500 μM IPTG overnight at 30 °C, stained with DAPI, and examined by fluorescence microscopy. In cells stained with DAPI, poly(P) appears yellow or orange, and DNA appears blue. At least 200 randomly selected cells were analyzed in each case. Proportions of cells with normal morphology showing polar (P), diffuse (D), or no detectable fluorescence above background (N) are indicated to the right.
(A) Poly(P) localization in WT, gppA, ppx, and ppk disruptants.
(B) Poly(P) localization in uhpT, wcaK, ynbC, and zntR disruptants.
(C) Selected examples of cells showing poly(P) and GFP/LtrA colocalization.
Bar = 2 μm.
doi:10.1371/journal.pbio.0060150.g006

RTs, although these enzymes appeared somewhat less sensitive to poly(P) inhibition than LtrA (Figure 7C and 7D). Together, the above findings show that poly(P) binds LtrA and inhibits its RT activity. The ability of poly(P) to bind LtrA and carry it toward the opposite pole in a non-denaturing gel supports its hypothesized mechanism of action in the cell.

The gppA and ppx Disruptants Show Altered Localization of Other Basic Proteins

Finally, we used the gppA and ppx disruptants to test whether poly(P) accumulation might similarly affect the polar localization of proteins other than LtrA. First, we tested GFP fusions of two basic proteins, which were shown previously to be pole-localized in E. coli: the N. crassa CYT-18 protein (calculated pI = 9.29) [12] and the E. coli transcriptional regulator XapR (calculated pI = 8.91) [34]. Strikingly, we found that both proteins are largely pole-localized in wild type and the ppk disruptant but showed more dispersed localization patterns in the gppA and ppx disruptants, which accumulate poly(P) (Figure 8A and 8B). For GFP/CYT-18, the gppA and ppx disruptants showed high proportions of cells with more diffuse protein localization, while for GFP/XapR these disruptants showed high proportions of cells with multiple large foci scattered throughout the cell. For GFP/XapR, we confirmed by dual-fluorescence microscopy that

the scattered localization in individual cells is again correlated with the accumulation and dispersal of poly(P) (86% of the gppA and 83% of the ppx cells showing scattered GFP/XapR localization also showed dispersed poly(P) localization). Immunoblots showed that GFP/XapR is expressed at similar levels in the wild-type and gppA and ppx disruptant strains (Figure S6).

By contrast to these basic proteins, a GFP fusion with a S. flexneri IcsA protein subsegment (IcsA$_{507-620}$ pI = 7.15) [35] remained pole-localized in the gppA and ppx disruptants, although for both mutants an increased proportion of cells with pole-localized IcsA$_{507-620}$/GFP showed additional tiny foci distributed throughout the cell (P*; Figure 8C). Thus, as expected, poly(P) accumulation most strongly affects the localization of positively charged proteins to which it can bind directly.

Discussion

Here, by using high-throughput methods to screen a transposon-insertion library, we identified five E. coli genes (gppA, uhpT, wcaK, ynbC, and zntR) whose disruption affects the polar localization of LtrA, a group II intron-encoded reverse transcriptase that functions with the intron RNA in RNPs to promote intron mobility. All of the above disruptants show both an increased proportion of cells with more
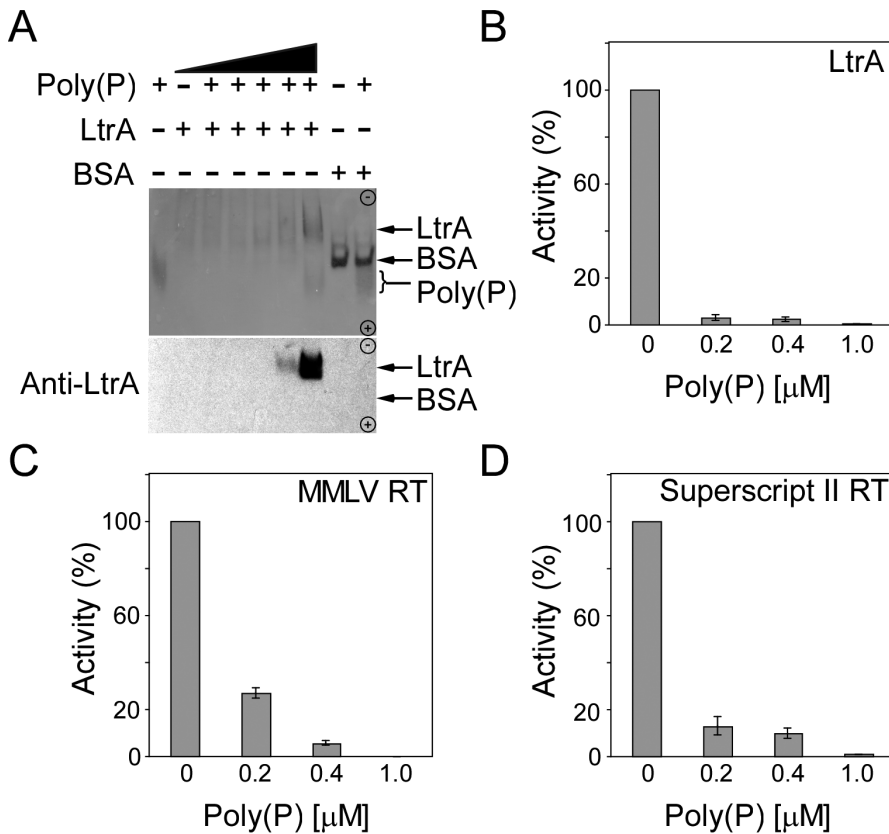
Figure 7. Poly(P) Binds to LtrA and Inhibits its RT Activity

(A) Nondenaturing PAGE. LtrA protein (100 pmol) by itself or mixed with different amounts of poly(P) (1 pmol, 10 pmol, 100 pmol, 1 nmol, and 10 nmol) was run in a nondenaturing 5–15% polyacrylamide gradient gel. Bovine serum albumin (100 pmol; BSA) by itself or mixed with10 nmol poly(P) was run in parallel lanes. The gel was silver-stained, and a parallel gel (below) was blotted to nitrocellulose and probed with anti-LtrA antibody (see Materials and Methods section).

(B–D) RT assays. RT activity was assayed by incubating 200 nM LtrA or dilutions of Moloney murine leukemia virus or Superscript II RT (Invitrogen) having equivalent activity with $[^{32}P]$-dTTP and poly(rA)/oligo(dT)$_{18}$ in reaction medium containing 10 mM KCl, 10 mM MgCl$_2$, and 50 mM Tris-HCl, pH 7.5, for 10 min at 37 °C in the presence or absence of 0.2, 0.4, or 1 μM poly(P). Polymerization of $[^{32}P]$-dTTP was measured as described in the Materials and Methods section and [50]. For all three enzymes, RT activities were 20,000–100,000 cpm, and incubation times were verified to be in the linear range. The bar graphs show the mean activity for three independent determinations, with the error bars indicating the standard deviation.
doi:10.1371/journal.pbio.0060150.g007

diffuse GFP/LtrA localization and a more uniform genomic distribution of Ll.LtrB-insertion sites, which in the wild-type *E. coli* strain are strongly clustered in the *oriC* region. These findings indicate that the intracellular localization of LtrA is a major determinant of Ll.LtrB-insertion-site preference, to our knowledge the first such demonstration for any mobile genetic element. Further analysis showed that the common factor leading to more diffuse GFP/LtrA localization in these and other disruptants is the accumulation of intracellular poly(P) and that disruptants that accumulate poly(P) also show altered intracellular distributions of other basic proteins that are normally pole-localized (CYT-18 and XapR). The latter findings suggest that poly(P) accumulation may be part of a cellular mechanism that leads to relocalization of basic proteins in response to cell stress or entry into stationary phase. From a technical standpoint, our results demonstrate the feasibility of using bacterial cellular arrays for high-throughput screens to identify mutations affecting protein localization or morphology, and they suggest a method for obtaining more uniform group II intron-gene disruption libraries by using mutants that accumulate poly(P).

The polar localization of LtrA in wild-type cells may

facilitate group II intron mobility by increasing access of group II intron RNPs to exposed DNA segments in the *oriC* and *ter* regions of the *E. coli* chromosome. It also may provide favorable sites for interaction with DNA replication components and a means of coordinating group II intron mobility with DNA replication and/or cell division [12]. Other mobile elements use a variety of mechanisms for coordinating transposition with DNA replication ([36,37] and references therein). Such coordination may be particularly important for group II introns, which can use nascent strands at DNA replication forks to prime reverse transcription [11,38,39]. Indeed, Coros et al. [11] found that in *E. coli* the frequency of Ll.LtrB retrotransposition events that use this priming mechanism is highest in the *oriC* domain and decreases in a gradient toward the *ter* domain, while retrotransposition events that utilize the DNA cleavage activity of the IEP to generate the primer for reverse transcription do not show such a gradient. The selection for polar localization may have originated with ancestral group II introns whose IEPs lacked DNA cleavage activity and relied entirely on nascent DNA strands as primers.

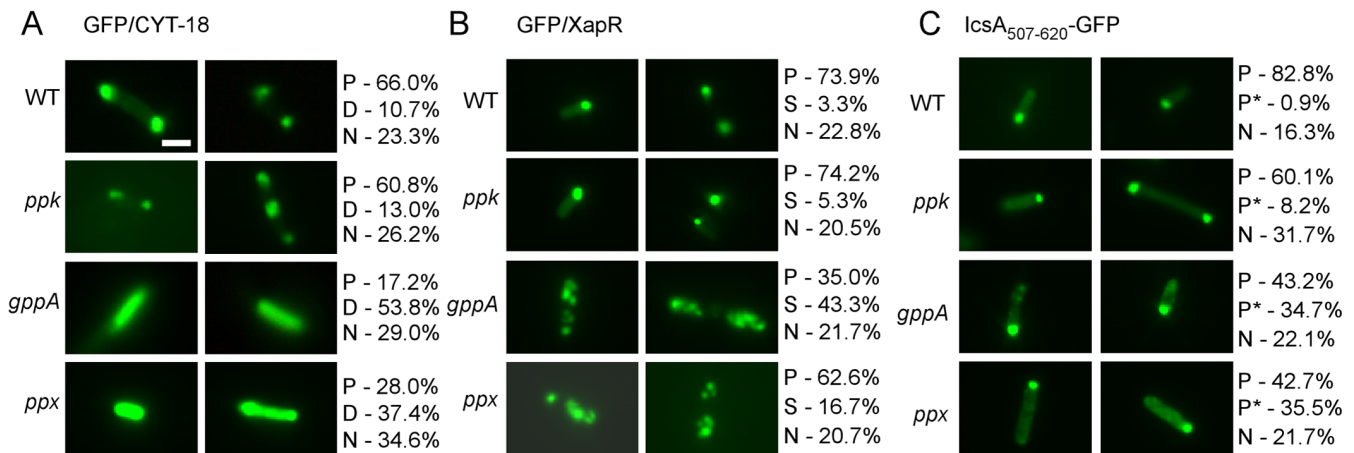In addition to changing the intracellular localization of

Figure 8. Disruptants that Accumulate Poly(P) Show Altered Intracellular Localization of Other Basic Proteins

Fluorescence microscopy of wild-type HMS174(DE3) (WT) and the indicated disruptants containing (A) pAC-GFP/CYT-18, (B) pAC-GFP/XapR, or (C) pBAD24-icsA$_{507-620}$::gfp. Cells were induced with (A and B) 500 μM IPTG or (C) 0.2% L-arabinose overnight at 30 °C. At least 200 cells were examined in each case, and the proportions of cells showing polar (P), diffuse (D), scattered (S), polar and dispersed tiny foci (P*), or no detectable poly(P) fluorescence above background (N) are indicated to the right. The localization patterns shown in the figure represent the most common pattern for each strain. Bar = 2 μm.

doi:10.1371/journal.pbio.0060150.g008

LtrA, poly(P) also potentially could affect the genomic distribution of Ll.LtrB-insertion sites by binding basic nucleoid-associated proteins, leading to nucleoid decondensation, as observed in a *Pseudomonas aeruginosa ppk1* mutant [40]. Indeed, it has been speculated that such a mechanism contributes to global changes in gene expression accompanying poly(P) accumulation in response to cell stress or entry into stationary phase [41]. However, Beauregard et al. [15] found that neither LtrA localization nor the distribution of Ll.LtrB-insertion sites is affected significantly by mutations in the nucleotide-associated proteins H-NS, StpA, or MukB, which lead to nucleoid decondensation in different ways. These findings indicate that nucleoid decondensation does not by itself lead to a more uniform distribution of Ll.LtrB-insertion sites as long as LtrA remains pole-localized. It is possible, however, that nucleotide decondensation contributes to the more uniform distribution of insertion sites that we observe when LtrA has been delocalized by poly(P).

Our results suggest that negatively charged poly(P) delocalizes LtrA and other basic proteins by binding to them directly. A direct binding mechanism is supported by: (i) the colocalization of GFP/LtrA and poly(P) in high proportions of *gppA* and *ppx* disruptant cells (Figure 6C); (ii) the finding that poly(P) accumulation affects the polar localization of three basic proteins (LtrA, CYT-18, and XapR) but not the polar localization of the acidic protein IcsA$_{507-620}$/GFP (Figure 8); and (iii) biochemical experiments showing that poly(P) can bind LtrA to inhibit its RT activity and cause it to migrate toward the opposite pole in a nondenaturing polyacrylamide gel (Figure 7). The binding of poly(P) to LtrA and other basic proteins is presumably nonspecific, but we cannot at this stage exclude a more specific binding component in some cases. In the cell, poly(P) may bind to LtrA and other basic proteins at the poles and relocalize them as it moves through the cell, and/or it may bind to the nascent proteins in other regions, preventing them from becoming pole-localized. The poly(P) that colocalizes with LtrA could be present in specific complexes, akin to volutin granules, which may be passively or actively localized or delocalized.

In addition to affecting the intracellular localization of LtrA, the binding of poly(P) may directly affect LtrA's biochemical activities in RNA splicing and intron mobility. Precedents for such effects include the findings that poly(P) activates Lon protease degradation of ribosomal proteins [42], may play a role in activating mammalian TOR kinase [43], and is required for the lytic growth of phages P1 and fd [44]. Our finding that poly(P) inhibits LtrA's RT activity (Figure 7B) may explain why the *ppk* mutant, which has decreased levels of poly(P), shows increased Ll.LtrB mobility frequencies in a chromosomal *lacZ* gene integration assay (Figure 5B). However, we also find that Ll.LtrB mobility frequencies are increased moderately in *gppA*, *ppx*, and other mutants that accumulate poly(P) (Figures 3A and 5B). The latter findings indicate that inhibition of LtrA's RT activity by poly(P) in vivo must be either mild or transient, perhaps due to dissociation or degradation of the bound poly(P) after the protein has been delocalized. A factor that may contribute to the moderately increased Ll.LtrB mobility frequencies in mutants that accumulate poly(P) is that their more uniform intracellular distribution of LtrA makes it easier to target the *lacZ* gene, which is located outside the *oriC* or *ter* chromosomal regions.

The disruptants that we identified with altered GFP/LtrA localization patterns accumulate poly(P) for different reasons. The *gppA* and *ppx* disruptions inhibit poly(P) degradation, while the *uhpT*, *wcaK*, *ynbC*, and *zntR* disruptants presumably accumulate poly(P) as a result of cellular stress caused by the disruptions. All of disruptants, including the *gppA* and *ppx* disruptants, have heterogeneous cellular phenotypes, with an increased proportion of cells showing both poly(P) accumulation and altered GFP/LtrA localization, and the remainder having wild-type localization patterns. This heterogeneity may reflect that only some cells in the population are under sufficient stress to trigger poly(P) accumulation. The wild-type strain shows similar heterogeneity but with only a small proportion of cells showing poly(P) accumulation and altered GFP/LtrA localization. Thus, the disruptions appear to increase the normal propensity for

stress-induced poly(P) accumulation, either by increasing the degree of stress or by decreasing the degradation rate of poly(P), making it easier to achieve elevated poly(P) concentrations. We note that the *gppA* disruption causes a more extreme accumulation and dispersal of poly(P) than does the *ppx* disruptant (Figure 6), possibly reflecting that the *gppA* disruptant not only lacks GPPA, which contributes to poly(P) degradation, but also accumulates pppGpp, which inhibits the remaining exopolyphosphatase PPX [42].

Like a previous screen for *E. coli* localization factors [16], our cell array screen did not identify a pole-localized receptor protein whose absence leads to diffuse LtrA localization. It is possible that a specific polar receptor for LtrA does not exist and that LtrA is localized to the poles by default because it is not actively localized elsewhere. Alternatively, the receptor may require essential proteins or be redundant or nonspecific (e.g., acidic phospholipids [45]). Additionally, the intriguing finding that in wild-type *E. coli* poly(P) detected by DAPI staining is found frequently in discrete foci at the poles raises the possibility that poly(P) itself contributes as a receptor for the polar localization of basic proteins under nonstress conditions. The finding that GFP/LtrA and other basic proteins remain pole-localized in *ppk* mutants, which have ~10-fold decreased poly(P) levels [27], does not exclude this possibility because poly(P) may be present in excess in wild-type strains and the residual poly(P) in the mutant may be sufficient for protein localization.

Finally, the finding that disruptants that accumulate poly(P) show altered distributions not only of LtrA but also of other pole-localized basic proteins suggests that poly(P) accumulation may be part of a mechanism that relocalizes proteins to different sites of action in response to cellular stress. One can imagine that reservoirs of certain enzymes, such as transcription factors or DNA repair enzymes, accumulate at the cellular poles and are mobilized to new sites of action by poly(P) during entry into stationary phase or under stress conditions, as shown here for LtrA. Such relocalization may be particularly advantageous when the cell's biosynthetic capacity is impaired as it is faster and more economical than synthesizing a specific receptor and transport system for each protein. Protein relocalization by binding to poly(P) may have wide physiological consequences, not only in prokaryotes but also in eukaryotes, where poly(P) also exists but has remained enigmatic.

Materials and Methods

Bacterial strains and growth conditions. *E. coli* HMS174(DE3) (F⁻ *recA hsdR rif*^{R}) (Novagen) was used for LtrA localization and Ll.LtrB intron-integration assays; DH5α was used for cloning; and S17–1λ*pir* [46] (obtained from Ram Narayanaswamy and Andy Ellington, University of Texas at Austin) was used for *mariner* transposon mutagenesis. Derivatives of HMS174(DE3) with disruptions of the *ppk*, *ppx*, and *relA* genes were constructed by targetron mutagenesis, as described ([8]; Figure S5). Keio deletion strains obtained from GenoBase (http://ecoli.naist.jp/GB6/search.jsp) were *ppk*, *ppx*, *uhpT*, *wcaK*, *ynbC*, and *zntR*. Other mutants obtained from GenoBase were *gppA* and *relA/spoT*. GenoBase strains were lysogenized with λ(DE3) carrying an IPTG-inducible T7 RNA polymerase gene by using a kit (Novagen) and are indicated with an asterisk in the text to denote their different genetic background. Strains were grown in LB medium at 30 or 37 °C, with antibiotics used at the following concentrations: ampicillin, 100 µg/ml; chloramphenicol, 25 µg/ml; kanamycin, 40 µg/ml; rifampicin, 100 µg/ml; trimethoprim, 10 µg/ml.

Recombinant plasmids. pACD2X-GFP/LtrA expresses the Ll.LtrB-ΔORF intron and a GFP fusion protein (Figure 1A) [12]. The pACD3-Tp^R-RAM library expresses Ll.LtrB-ΔORF introns with randomized EBS2, EBS1, and δ sequences plus a Tp^R-RAM for detecting chromosome integrations [10]. Plasmids expressing other GFP fusion proteins were: pAC-GFP/CYT-18, *N. crassa* CYT-18 protein with an N-terminal GFP fusion [12]; pBAD24-*icsA*$_{507-620}$::*gfp*, pole-localized segment of the *S. flexneri* IcsA protein with a C-terminal GFP fusion [35]; and pAC-GFP/XapR, *E. coli* XapR protein with an N-terminal GFP fusion. The latter plasmid was derived from pAC-GFP/LtrA [12] by replacing the LtrA ORF with the *xapR* ORF (codons 1–294) amplified from *E. coli* HMS174(DE3) by PCR. pSC189 expresses a *mariner* transposon with a *kan*^{R} marker and a separately encoded hyperactive C9 transposase [47]. The protein expression plasmid pImp-1P contains the LtrA ORF cloned behind a *tac* promoter in pCYB2 (New England Biolabs) [4].

Construction of a *mariner* transposon-insertion library. *E. coli* strains HMS174(DE3) and S17–1λ*pir* carrying pSC189 (see above) were grown separately to OD$_{600}$ = 0.5 at 37 °C in 10 ml of LB without and with ampicillin, respectively, then mixed, and incubated at room temperature overnight without shaking for conjugation. The conjugated cells were washed twice with LB medium by centrifugation, resuspended, and grown overnight at 37 °C in fresh LB medium containing rifampicin and kanamycin to kill the donor strain and select for recipient HMS174(DE3) cells containing *mariner* transposon insertions. Loss of pSC189, which carries an *amp*^{R} marker and does not replicate in HMS174(DE3), was confirmed by plating on LB agar with and without ampicillin (<1% Amp^R colonies). The HMS174(DE3) isolate used for library construction inadvertently carried a Tet^R broad-host-range plasmid pBBR1MCS-3 [48]. For the GFP/LtrA localization screen, cells grown in LB with kanamycin were electroporated with the intron-donor plasmid pACD2X-GFP/LtrA and plated on LB agar containing chloramphenicol and kanamycin. Approximately 9,600 colonies were picked into one hundred 96-well plates and stored at −80 °C. TAIL PCR of isolates showed that >92% contained different *mariner* transposon insertions, both before and after introduction of pACD2X-GFP/LtrA.

Cell microarray construction and imaging. The *E. coli* HMS174(DE3) *mariner* transposon-insertion library carrying pACD2X-GFP/LtrA was inoculated into new 96-well plates containing LB medium with chloramphenicol plus kanamycin and incubated overnight at 37 °C. The cultures then were inoculated 1:10 into fresh medium plus 17% glycerol in a new 96-well plate and grown for 5 h at 37 °C. In one screen, cells in fifty-one 96-well plates were induced overnight with 100 µM IPTG at 37 °C, and in another screen, cells in forty-nine 96-well plates were induced overnight with 500 µM IPTG at 30 °C. Culture transfer and media additions were done by a Biomek FX Laboratory Automation Workstation (Beckman Coulter).

Cell microarrays (cell chips) were constructed as described [17]. Briefly, ~5,000 knockouts plus a wild-type HMS174(DE3) control were printed onto poly-L-lysine-coated microscope slides using a custom-built DNA microarray-printing robot. In each experiment, ~30 cell chips were made, of which two were used for imaging and the remainder were stored at −80 °C. Before being imaged, the cell chips were washed briefly with double-distilled water to remove glycerol and debris and then mounted with VECTASHIELD hard-set mounting medium containing 1.5 µg/ml DAPI. Cell images were collected by automated microscopy, using a Nikon E800 fluorescence microscope with computer-controlled *X-Y* stage and piezoelectric-positioned objective. The automated microscope scanned the position of each spot, focused, and captured the image with a Coolsnap CCD camera (Photometrics). Images were stored in a custom cell microarray image database (Cellma, http://cellma.icmb.utexas.edu/) and examined individually to identify strains with altered GFP/LtrA localization patterns.

Fluorescence microscopy. Fluorescence microscopy was done as described [12]. Cells carrying pACD2X-GFP/LtrA were grown in LB medium with appropriate antibiotics at 37 °C to OD$_{600}$ = 0.3 and then induced overnight with 500 µM IPTG at 30 °C or 100 µM IPTG at 37 °C. DAPI (25 µg/ml) was added to cultures 30 min before the end of induction. Cells were examined by fluorescence microscopy using a Leica DMIRBE microscope (Leica) with a 100× oil lens (PL APO 1.4–0.7 NA) and a GFP filter for GFP fluorescence or a wide DAPI filter for poly(P) fluorescence. Photographs were taken with a Leica DFC350 FX fluorescence camera (GFP fluorescence) or a Leica DFC320 FX color camera (poly(P) fluorescence).

Intron mobility assays. Ll.LtrB-ΔORF intron mobility frequencies were determined by using a retargeted intron that inserts at a site within the *E. coli lacZ* gene (targetron LacZ-1063a; Figure S5). Cells containing the retargeted intron cloned in pACD2X were grown in LB medium with chloramphenicol at 37 °C to OD$_{600}$ = 0.2–0.3 and induced with 500 µM IPTG for 0.5 h at 30 °C or 100 µM IPTG for 1 h

at 37 °C. The cells then were washed with fresh LB medium and plated on LB containing X-Gal (Fisher Scientific). After overnight incubation at 37 °C, the *lacZ* integration frequency was calculated as the percentage of white colonies.

Chromosomal distribution of Ll.LtrB-insertion sites. Cells transformed with a pACD3-Tp[R]-RAM library of Ll.LtrB introns with randomized EBS2, EBS1, and δ sequences and a Tp[R]-RAM inserted in intron domain IV [10] were grown overnight at 37 °C in LB medium containing chloramphenicol (wild-type strains) or chloramphenicol plus kanamycin (disruptants), then inoculated 1:100 into fresh medium, grown to OD_{600} = 0.3, and induced with 500 μM IPTG overnight at 30 °C. Cells containing chromosomally integrated Ll.LtrB introns carrying the activated Tp[R]-RAM were selected by plating on Mueller–Hinton medium with trimethoprim and thymine [10].

Thermal-asymmetric-interlaced PCR. TAIL PCR [49] was done on colonies resuspended in PCR premix. Integration junctions were amplified by two successive PCRs, using two nested specific primers in combination with a single degenerate primer. For *mariner* transposon insertions, the first PCR used the specific primer TailP1 (5′-GTTCTTCTGAGCGGGACTCTGGGG-3′) and the degenerate primer AD2 (5′-NGTCGASWGANAWGA-3′, where N = A, C, G, or T; S = C or G; and W = A or T), and the second PCR used the specific primer TailP2 (5′-CGGCCGCGAAGTTCCTATTCCG-3′) and AD2. The final PCR product was gel-purified and sequenced using the TailP2 primer. For Ll.LtrB-intron insertions, the specific primers used in the first and second PCRs were Ell1 (5′-CTGATTAACATTGCGACTCAGTCG-TACCC-3′) and Ell2 (5′-CAACCGTGCTCTGTTCCCGTATCAG-3′), respectively, and the degenerate primer was again AD2. The final PCR products were sequenced by using primer Ell3 (5′-GGTTGGCTGTTTTCTGTGTTATCTTACAGAG-3′).

SDS-PAGE and immunoblotting. Proteins isolated from equal amounts of cells (OD_{600} = 0.02 or 0.04) were run in either a 7.5% polyacrylamide/0.1% SDS gel (GFP/LtrA, Figure S3) or a 10% polyacrylamide/0.1% SDS gel (LtrA, Figures 3 and 5; GFP/XapR, Figure S6), then transferred to a nitrocellulose membrane (Bio-Rad) by using a semidry transfer apparatus (Hoefer Semiphor TE 70; Amersham Biosciences). The blots were probed with a 1:5,000 dilution of anti-GFP antibody JL-8 (BD Biosciences), followed by a 1:10,000 dilution of horseradish peroxidase goat anti-mouse secondary antibody (Bio-Rad), or with a 1:1,000 dilution of an anti-LtrA antibody preparation (obtained from Gary Dunny, University of Minnesota), followed by a 1:100,000 dilution of horseradish peroxidase goat anti-rabbit secondary antibody (Pierce). Blots were developed with Amersham ECL western blotting detection reagents (GE Healthcare). Equal loading was confirmed by Coomassie blue staining of a parallel gel.

Southern hybridization. DNA was isolated from wild-type and mutants strains by using a genomic DNA isolation kit (Qiagen), digested with restriction enzymes, and run in a 0.8% agarose gel. The gel was blotted to a nylon transfer membrane (Magna, 0.45 μm; GE Osmonics Labstore) and hybridized with a ^{32}P-labeled probe corresponding to *mariner* transposon positions 1385–1868. The probe was generated by PCR of pSC189 with primers Mar3200 (5′-GGGTGGGAGAGGCTATTCGGCTATGACTGGGC-3′) and Mar-3650 (5′-CCTTGAGCCTGGCGAACAGTTCGGCTGG-3′), followed by labeling with [α-^{32}P]dTTP (3,000 Ci/mmol; PerkinElmer), using a High Prime DNA labeling kit (Roche). The blots were scanned with a Typhoon Trio fluorescence scanner (Amersham Biosciences).

Nondenaturing PAGE and RT assays. The LtrA protein was expressed in *E. coli* Rosetta(DE3) (Novagen) from the intein-based expression plasmid pImp-1P (see above) and purified, essentially as described [4]. The LtrA protein used for RT activity assays was purified through an additional heparin-Sepharose chromatography step. For nondenaturing PAGE, poly(P) (Type 65; Sigma-Aldrich) was incubated with purified LtrA protein and bovine serum albumin (Fraction V (Sigma-Aldrich), with 20% glycerol added to match LtrA) in 20 μl of 100 mM KCl, 5 mM $MgCl_2$, 20 mM Tris-HCl, pH 7.5, for 30 min at 30 °C. The samples were then run in a nondenaturing 5–15% polyacrylamide gradient gel in Tris-acetate, pH 6.5, buffer. The gel was silver-stained, and a parallel gel was used for immunoblotting with anti-LtrA antibody (see above). RT activity was assayed as described [50] by polymerization of [^{32}P]-dTTP (3,000 Ci/mmol; PerkinElmer) with poly(rA)/oligo(dT)$_{18}$ as template in reaction medium containing 10 mM KCl, 10 mM $MgCl_2$, and 50 mM Tris-HCl, pH 7.5, for 10 min at 37 °C. Samples were spotted onto DE-81 paper (Whatman), washed three times with 2× SSC (SSC is 0.15 M NaCl and 0.15 M citric acid, pH 7.0.), and counted in a scintillation counter.

Supporting Information

Figure S1. Confirmation of *mariner* Transposon-Insertion Sites by PCR Analysis of the 5′- and 3′-Integration Junctions

DNA isolated from the indicated disruptants by using a Genomic DNA Isolation Kit (Qiagen) was used as a template for PCR amplification of the 5′ (left) and 3′ (right) junctions of the inserted *mariner* transposon. The junction sequences were determined by sequencing the PCR products. The 5′ junction was amplified using primers P1 and P2, and the 3′ junction was amplified using primers P3 and P4. The gene-specific primers P1 and P4 were: *gppA*, gppA580 (5′-CAGTGTATGACCCTGGCGGGCGG-3′) and gppA-3end (5′-GCGTCAGCATCGCATCCGGCAC-3′); *uhpT*, uhpT1270 (5′-GGCTGGGCAGGCACCTTCGCCGCGC-3′) and ade1550 (5′-TGCCGTTACCCATTGCCGGGCTGATGAGC-3′); *wcaK*, wcaK50 (5′-GGGCAACCACACTTGCGGCAATCG-3′) and wcaK-350 (5′-CCTGATGCTGGTAGCGGCGAGG-3′); *ynbC*, ynbC990 (5′-TTGTTCGGGACGCACTCTTCGGGCTGC-3′) and ynbC-1670 (5′-TCACGCACGAGTGAATCCATCTCCCC-3′); *zntR*, zntR-420 (5′-CCACTCTTAACGCCACTCGCCCCTTGTTC-3′) and yhdN30 (5′-GGCAGAGCGCCATATAGCAGAAGCGC-3′). The *mariner* primers P2 and P3 were: Mar-2520 (5′-GCTTCTCAGTGCGTTA-CATCCCTGGC-3′) and TAILP2 (5′-CGGCCGCGAAGTTCCTAT-TCCG-3′), respectively. The Figure shows PCR products run in a 1% agarose gel, which was stained with ethidium bromide. M, 1-kb DNA ladder (Invitrogen).

Found at doi:10.1371/journal.pbio.0060150.sg001 (5.2 MB TIF).

Figure S2. Confirmation of *mariner* Transposon-Insertion Sites by Southern Hybridization

Genomic DNA (10 μg) from wild-type *E. coli* HMS174(DE3) (WT) and the indicated disruptants was digested with XcmI, XmaI, and SacII (60 units each, overnight, at 37 °C) and run in a 0.8% agarose gel. The gel was blotted to a nylon membrane (Magna, 0.45 μm; GE Osmonics Labstore) and hybridized with a ^{32}P-labeled probe corresponding to *mariner* transposon positions 1385–1868 (see Materials and Methods section). The blot was dried and scanned with a Typhoon Trio phosphorimager (Amersham Biosciences). M, 1-kb plus DNA ladder (Invitrogen).

Found at doi:10.1371/journal.pbio.0060150.sg002 (4.5 MB TIF).

Figure S3. Immunoblots of GFP/LtrA Expressed from pACD2X-GFP/LtrA in Wild Type and Disruptants

Samples were from fluorescence microscopy experiments in which wild-type HMS174(DE3) (WT) and the indicated disruptants containing pACD2X-GFP/LtrA were induced with 500 μM IPTG at 30 °C (Figures 2 and 5). Top, immunoblots of GFP/LtrA probed with anti-GFP antibody (JL-8; BD Biosciences). Bottom, parallel gels stained with Coomassie blue. Arrows to the left of the gel indicate positions of size markers (Kaleidoscope Prestained Standard; Bio-Rad). Independent repeats of the experiment gave similar results. In one experiment, the GFP/LtrA expression level in the *gppA* disruptant appeared slightly higher than that in the wild type.

Found at doi:10.1371/journal.pbio.0060150.sg003 (3.6 MB TIF).

Figure S4. PCR Analysis of Disruptants Containing *mariner* Transposon Insertions Using Primers Flanking the Disrupted Genes

PCRs were done on genomic DNA isolated from each strain with an annealing temperature of 60 °C, using the following P1 and P2 primers specific for each gene: *gppA*, gppA1440 (5′-CGTGCCAGA-GATGACATTACAGGCTAACC-3′) and gppA-1600 (5′-GATGCGT-CAGCATCGCATCCGGCAC-3′); *uhpT*, uhpT1310 (5′-GCCAAGTTAGGTCTGGGAATGATTGCCG-3′) and uhpT-1560 (5′-GGCGAGAAGTTTGCCTTCACTACGCTGG-3′); *wcaK*, wcaK50 and wcaK-350 (Figure S2); *ynbC*, ynbC990 and ynbC-1670 (Figure S2); *zntR*, zntR-420 and yhdN30 (Figure S2). The PCR products were run in a 1% agarose gel, which was stained with ethidium bromide. M, 1-kb DNA ladder (Invitrogen). The prominent smaller band in the lane for the *gppA* disruptant contains primer dimers. The light band that comigrates with the wild-type band in the *zntR* disruptant (star) has a 4-bp insertion (ACAG) at the mariner transposon-insertion site (nucleotide position 171 counting from the A of the ATG initiation codon). This band presumably results from transposon excision and was found in multiple repeats with individual *zntR* disruptant colonies. Analogous bands due to transposon excision were not seen in the other disruptants.

Found at doi:10.1371/journal.pbio.0060150.sg004 (5.3 MB TIF).

Figure S5. DNA Target Site Sequences and Base-Pairing Interactions for Targetrons Used for Gene Disruptions

Retargeted Ll.LtrB-ΔORF introns (targetrons) are designated by a number that corresponds to the nucleotide position 5′ to the insertion site in the target gene's coding sequence, followed by "a" indicating the antisense strand. DNA target sequences are shown from positions −30 to +15 from the intron-insertion site, with nucleotide residues that match those in the wild-type Ll.LtrB intron target site highlighted in gray in the top strand. The intron-insertion site (IS) in the top strand and the IEP cleavage site (CS) in the bottom strand are indicated by arrowheads. Targetron LacZ-1063a was expressed from pACD2X [51], and targetrons Ppk-1140a, Ppx-1051a, and RelA-733a were expressed from pACD-Kan^R-RAM. The latter plasmid is a derivative of pACD2X in which the Ll.LtrB-ΔORF intron contains a modification of a previously constructed kan^R retrotransposition-indicator gene [52] inserted at the MluI site in intron domain IV. Targetrons were used for *E. coli* gene disruption as described ([8], see also http://www.sigmaaldrich.com/Area__of__Interest/Life__Science/Functional__Genomics__and__RNAi/TargeTron.html). Prior to analysis of the disruptants, the pACD-Kan^R-RAM donor plasmid, which carries a cap^R marker on the vector backbone, was cured by transforming the strain with an incompatible Amp^R plasmid pACYC177, followed by growth on LB medium containing ampicillin. Targetron disruptions were confirmed by PCR and sequencing across the targetron-integration junctions and by Southern hybridization to verify a single targetron integration at the desired site (unpublished data).

Found at doi:10.1371/journal.pbio.0060150.sg005 (5.3 MB TIF).

Figure S6. Immunoblots of GFP/XapR Fusion Protein Expressed from pAC-GFP/XapR in Wild-Type and Disruptants

Protein samples were from a fluorescence microscopy experiment in which wild-type HMS174(DE3) (WT) and disruptants were induced overnight with 500 μM IPTG at 30 °C (Figure 8). Top, immunoblot of GFP/XapR probed with anti-GFP antibody (JL-8; BD Biosciences). Bottom, parallel gel stained with Coomassie blue. Arrows to the left of the gel indicate positions of size markers (Kaleidoscope Prestained Standard; Bio-Rad). Quantitation of the immunoblot showed that the relative intensities of the GFP/XapR band in the WT, *gppA*, *ppk*, and *ppx* lanes are 1:1.05:0.61:1.07. In an independent repeat of the experiment, the relative intensities were 1:1.35:0.35:0.88.

Found at doi:10.1371/journal.pbio.0060150.sg006 (2.2 MB TIF).

Table S1. GFP/LtrA Localization in Wild Type and Disruptants at 37 °C

Found at doi:10.1371/journal.pbio.0060150.st001 (36 KB DOC).

Accession Numbers

Accession numbers for Keio deletion strains from GenoBase (http://ecoli.naist.jp/GB6/search.jsp) are *ppk* (JW2486), *ppx* (JW2487), *uhpT* (JW3641), *wcaK* (JW2030), *ynbC* (JW1407), *zntR* (JW2354), *gppA* (JD24693), and *relA/spoT* (AQ4319).

References

1. Lambowitz AM, Zimmerly S (2004) Mobile group II introns. Annu Rev Genet 38: 1–35.
2. Pyle AM, Lambowitz AM (2006) Group II introns: ribozymes that splice RNA and invade DNA. In: Gesteland RF, Cech TR, Atkins JF, editors. The RNA World. 3rd Edition. New York: Cold Spring Harbor Laboratory Press. pp. 469–505.
3. Cousineau B, Smith D, Lawrence-Cavanagh S, Mueller JE, Yang J, et al. (1998) Retrohoming of a bacterial group II intron: mobility via complete reverse splicing, independent of homologous DNA recombination. Cell 94: 451–462.
4. Saldanha R, Chen B, Wank H, Matsuura M, Edwards J, et al. (1999) RNA and protein catalysis in group II intron splicing and mobility reactions using purified components. Biochemistry 38: 9069–9083.
5. Smith D, Zhong J, Matsuura M, Lambowitz AM, Belfort M (2005) Recruitment of host functions suggests a repair pathway for late steps in group II intron retrohoming. Genes Dev 19: 2477–2487.
6. Guo H, Karberg M, Long M, Jones JP III, Sullenger B, et al. (2000) Group II introns designed to insert into therapeutically relevant DNA target sites in human cells. Science 289: 452–457.
7. Mohr G, Smith D, Belfort M, Lambowitz AM (2000) Rules for DNA target-site recognition by a lactococcal group II intron enable retargeting of the intron to specific DNA sequences. Genes Dev 14: 559–573.
8. Perutka J, Wang W, Goerlitz D, Lambowitz AM (2004) Use of computer-designed group II introns to disrupt *Escherichia coli* DExH/D-box protein and DNA helicase genes. J Mol Biol 336: 421–439.
9. Karberg M, Guo H, Zhong J, Coon R, Perutka J, et al. (2001) Group II introns as controllable gene targeting vectors for genetic manipulation of bacteria. Nature Biotechnol 19: 1162–1167.
10. Zhong J, Karberg M, Lambowitz AM (2003) Targeted and random bacterial gene disruption using a group II intron (targetron) vector containing a retrotransposition-activated selectable marker. Nucleic Acids Res 31: 1656–1664.
11. Coros CJ, Landthaler M, Piazza CL, Beauregard A, Esposito D, et al. (2005) Retrotransposition strategies of the *Lactococcus lactis* Ll.LtrB group II intron are dictated by host identity and cellular environment. Mol Microbiol 56: 509–524.
12. Zhao J, Lambowitz AM (2005) A bacterial group II intron-encoded reverse transcriptase localizes to cellular poles. Proc Natl Acad Sci U S A 102: 16133–16140.
13. Niki H, Yamaichi Y, Hiraga S (2000) Dynamic organization of chromosomal DNA in *Escherichia coli*. Genes Dev 14: 212–223.
14. Bates D, Kleckner N (2005) Chromosome and replisome dynamics in *E. coli*:
loss of sister cohesion triggers global chromosome movement and mediates chromosome segregation. Cell 121: 899–911.
15. Beauregard A, Chalamcharla VR, Piazza CL, Belfort M, Coros CJ (2006) Bipolar localization of the group II intron Ll.LtrB is maintained in *Escherichia coli* deficient in nucleoid condensation, chromosome partitioning and DNA replication. Mol Microbiol 62: 709–722.
16. Nilsen T, Yan AW, Gale G, Goldberg MB (2005) Presence of multiple sites containing polar material in spherical *Escherichia coli* cells that lack MreB. J Bacteriol 187: 6187–6196.
17. Narayanaswamy R, Niu W, Scouras A, Hart GT, Davies J, et al. (2006) Systematic profiling of cellular phenotypes with spotted cell microarrays reveals new pheromone response genes. Genome Biol 7: R6.
18. Keasling JD, Bertsch L, Kornberg A (1993) Guanosine pentaphosphate phosphohydrolase of *Escherichia coli* is a long-chain exopolyphosphatase. Proc Natl Acad Sci U S A 90: 7029–7033.
19. Hall JA, Maloney PC (2001) Transmembrane segment 11 of UhpT, the sugar phosphate carrier of *Escherichia coli*, is an α-helix that carries determinants of substrate selectivity. J Biol Chem 276: 25107–25113.
20. Stevenson G, Andrianopoulos K, Hobbs M, Reeves PR (1996) Organization of the *Escherichia coli* K-12 gene cluster responsible for production of the extracellular polysaccharide colanic acid. J Bacteriol 178: 4885–4893.
21. Blattner FR, Plunkett G III, Bloch CA, Perna NT, Burland V, et al. (1997) The complete genome sequence of *Escherichia coli* K-12. Science 277: 1453–1474.
22. Newberry KJ, Brennan RG (2004) The structural mechanism for transcription activation by MerR family member multidrug transporter activation, N terminus. J Biol Chem 279: 20356–20362.
23. Keseler IM, Collado-Vides J, Gama-Castro S, Ingraham J, Paley S, et al. (2005) EcoCyc: a comprehensive database resource for *Escherichia coli*. Nucleic Acids Res 33: D334–D337.
24. Xiao H, Kalman M, Ikehara K, Zemel S, Glaser G, et al. (1991) Residual guanosine 3′,5′-bispyrophosphate synthetic activity of *relA* null mutants can be eliminated by *spoT* null mutations. J Biol Chem 266: 5980–5990.
25. Akiyama M, Crooke E, Kornberg A (1992) The polyphosphate kinase gene of *Escherichia coli*. J Biol Chem 267: 22556–22561.
26. Akiyama M, Crooke E, Kornberg A (1993) An exopolyphosphatase of *Escherichia coli*. J Biol Chem 268: 633–639.
27. Crooke E, Akiyama M, Rao NN, Kornberg A (1994) Genetically altered levels of inorganic polyphosphate in *Escherichia coli*. J Biol Chem 269: 6290–6295.
28. Hung C, Peccia J, Zilles JL, Noguera DR (2002) Physical enrichment of polyphosphate-accumulating organisms in activated sludge. Water Environ Res 74: 354–361.

29. Roinestad FA, Yall I (1970) Volutin granules in *Zoogloea ramigera*. Appl Microbiol 19: 973–979.

30. Aprea G, Mullan WMA, Mullan A, Murru N, Tozzi M, et al. (2005) Isolation of polyphosphate-accumulating lactic acid bacteria from natural whey starters. Milchwissenschaft 60: 256–258.

31. Pallerla SR, Knebel S, Polen T, Klauth P, Hollender J, et al. (2005) Formation of volutin granules in *Corynebacterium glutamicum*. FEMS Microbiol Lett 243: 133–140.

32. Kornberg A, Rao NN, Ault-Riché D (1999) Inorganic polyphosphate: a molecule of many functions. Annu Rev Biochem 68: 89–125.

33. Ault-Riché D, Fraley CD, Tzeng C, Kornberg A (1998) Novel assay reveals multiple pathways regulating stress-induced accumulations of inorganic polyphosphate in *Escherichia coli*. J Bacteriol 180: 1841–1847.

34. Kitagawa M, Ara T, Arifuzzaman M, Ioka-Nakamichi T, Inamoto E, et al. (2005) Complete set of ORF clones of *Escherichia coli* ASKA library (a complete set of *E. coli* K-12 ORF archive): unique resources for biological research. DNA Res 12: 291–299.

35. Charles M, Perez M, Kobil JH, Goldberg MB (2001) Polar targeting of *Shigella* virulence factor IcsA in enterobacteriacae and *Vibrio*. Proc Natl Acad Sci U S A 98: 9871–9876.

36. Hu YW, Derbyshire KM (1998) Target choice and orientation preference of the insertion sequence IS903. J Bacteriol 180: 3039–3048.

37. Peters JE, Craig NL (2001) Tn7 recognizes transposition target structures associated with DNA replication using the DNA-binding protein TnsE. Genes Dev. 15: 737–747.

38. Zhong J, Lambowitz AM (2003) Group II intron mobility using nascent strands at DNA replication forks to prime reverse transcription. EMBO J 22: 4555–4565.

39. Martínez-Abarca F, Barrientos-Durán A, Fernández-López M, Toro N (2004) The RmInt1 group II intron has two different retrohoming pathways for mobility using predominantly the nascent lagging strand at DNA replication forks for priming. Nucleic Acids Res 32: 2880–2888.

40. Fraley CD, Rashid MH, Lee SS, Gottschalk R, Harrison J, et al. (2007) A polyphosphate kinase 1 (*ppk1*) mutant of *Pseudomonas aeruginosa* exhibits multiple ultrastructural and functional defects. Proc Natl Acad Sci U S A 104: 3526–3531.

41. Brown MR, Kornberg A (2004) Inorganic polyphosphate in the origin and survival of species. Proc Natl Acad Sci U S A 101: 16085–16087.

42. Kuroda A, Murphy H, Cashel M, Kornberg A (1997) Guanosine tetra- and pentaphosphate promote accumulation of inorganic polyphosphate in *Escherichia coli*. J Biol Chem 272: 21240–21243.

43. Wang L, Fraley CD, Faridi J, Kornberg A, Roth RA (2003) Inorganic polyphosphate stimulates mammalian TOR, a kinase involved in the proliferation of mammary cancer cells. Proc Natl Acad Sci U S A 100: 11249–11254.

44. Li L, Rao NN, Kornberg A (2007) Inorganic polyphosphate essential for lytic growth of phages P1 and fd. Proc Natl Acad Sci U S A 104: 1794–1799.

45. Mileykovskaya E, Dowhan W (2005) Role of membrane lipids in bacterial division-site selection. Curr Opin Microbiol 8: 135–142.

46. Simon R, Priefer UB, Pühler A (1983) A broad host range mobilization system for *in vivo* genetic engineering: transposon mutagenesis in gram negative bacteria. Biotechnology 1: 784–791.

47. Chiang SL, Rubin EJ (2002) Construction of a *mariner*-based transposon for epitope-tagging and genomic targeting. Gene 296: 179–185.

48. Kovach ME, Elzer PH, Hill DS, Robertson GT, Farris MA, et al. (1995) Four new derivatives of the broad-host-range cloning vector pBBR1MCS, carrying different antibiotic-resistance cassettes. Gene 166: 175–176.

49. Liu YG, Whittier RF (1995) Thermal asymmetric interlaced PCR: automatable amplification and sequencing of insert end fragments from P1 and YAC clones for chromosome walking. Genomics 25: 674–681.

50. Matsuura M, Saldanha R, Ma H, Wank H, Yang J, et al. (1997) A bacterial group II intron encoding reverse transcriptase, maturase, and DNA endonuclease activities: biochemical demonstration of maturase activity and insertion of new genetic information within the intron. Genes Dev 11: 2910–2924.

51. San Filippo J, Lambowitz AM (2002) Characterization of the C-terminal DNA-binding/DNA endonuclease region of a group II intron-encoded protein. J Mol Biol 324: 933–951.

52. Ichiyanagi K, Beauregard A, Lawrence S, Smith D, Cousineau B, et al. (2002) Retrotransposition of the Ll.LtrB group II intron proceeds predominantly via reverse splicing into DNA targets. Mol Microbiol 46: 1259–1272.